Protoribosome by quantum kernel energy method

Lulu Huang[a], Miri Krupkin[b], Anat Bashan[b], Ada Yonath[b,1], and Lou Massa[c]

[a]Center for Computational Materials Science, Naval Research Laboratory, Washington, DC 20375-5341; [b]Department of Structural Biology, Weizmann Institute of Science, Rehovot 76100, Israel; and [c]Hunter College and the Graduate School, City University of New York, New York, NY 10065

Contributed by Ada Yonath, July 31, 2013 (sent for review May 11, 2013)

Experimental evidence suggests the existence of an RNA molecular prebiotic entity, called by us the "protoribosome," which may have evolved in the RNA world before evolution of the genetic code and proteins. This vestige of the RNA world, which possesses all of the capabilities required for peptide bond formation, seems to be still functioning in the heart of all of the contemporary ribosome. Within the modern ribosome this remnant includes the peptidyl transferase center. Its highly conserved nucleotide sequence is suggestive of its robustness under diverse environmental conditions, and hence on its prebiotic origin. Its twofold pseudosymmetry suggests that this entity could have been a dimer of self-folding RNA units that formed a pocket within which two activated amino acids might be accommodated, similar to the binding mode of modern tRNA molecules that carry amino acids or peptidyl moieties. Using quantum mechanics and crystal coordinates, this work studies the question of whether the putative protoribosome has properties necessary to function as an evolutionary precursor to the modern ribosome. The quantum model used in the calculations is density functional theory–B3LYP/3–21G*, implemented using the kernel energy method to make the computations practical and efficient. It occurs that the necessary conditions that would characterize a practicable protoribosome—namely (*i*) energetic structural stability and (*ii*) energetically stable attachment to substrates—are both well satisfied.

bonding apparatus | puromycin | interaction energy | self-assembly | chemical model

A suggestion of a molecular entity, called "protoribosome," which may have evolved and emerged from an RNA world before a subsequent evolution into the modern protein/nucleic acid world, has been reported (1–3). In contemporary cells the ribosomes translate the genetic information (stored in the DNA) into proteins. Ribosomes are gigantic complexes, which in prokaryotes are built of some 50 proteins and three RNA chains with a total of 4,500 nucleotides. Aptly referred to as the protein factory of all living cells, the ribosome is essential to the contemporary life, and its activity may have been crucial to the formation of life itself. Structural analysis identified an internal RNA region that exists in all known structures (1–5) and has universally conserved sequence (1), which contains the site of peptide bond formation, and thus may well be that of a remaining RNA world entity. Consistent with the findings that the main ribosomal functions—namely, the decoding of the genetic code, the formation of peptide bonds, and the creation of elongating proteins—are performed by ribosomal RNA and with the universality of this region among all kingdoms of life, we proposed that this region is a remnant of a prebiotic chemical entity with catalytic capabilities, and called it the "protoribosome." Within the otherwise asymmetric ribosome, this region has a unique fold (6) and could have been the link to the modern world (7). It is characterized by a pseudotwofold symmetry with a highly conserved nucleotide sequence and seems to possess all of the assumed prerequisites for the formation of chemical bonds. This semisymmetric object could be a dimer of self-folding RNA units that formed a pocket within which two activated amino acids, as substrates, might be accommodated.

A representation of a plausible sequence for spontaneous self-assembly of a protoribosome is shown in Fig. 1 (2). Here, we put forth the use of quantum mechanics to answer the following question: Is the suggested protoribosome structure a plausible reality? One may systematically remove—that is, mathematically—all surrounding parts of the modern ribosome and use the coordinates of a central symmetric pocket for constructing a putative protoribosome. Here we apply quantum mechanics to the structure of that protoribosome. The most fundamental inquiry followed in this article is that of the energetic stability of the proposed protoribosome. This is not presently known. And obviously if the structure is not energetically stable, it is not likely to be able to act as a biological catalyst, as would be required of a protoribosome. The protoribosome contains almost 200 nucleotides, namely thousands of atoms. Ab initio quantum calculations rise in difficulty as a high power of the number of atoms in the system. Therefore, quantum calculation of the protoribosome energy is a complex computational problem. Fortunately we are in possession of a recently discovered kernel energy method (KEM) (8–24), described below, which alleviates dramatically the computational difficulty of ab initio calculations. Importantly the KEM is highly accurate, as well as computationally efficient.

As an example of the large size of systems that can be studied with ab initio KEM, we have applied the method to a Hartree–Fock (HF) calculation of a 33,000-atom protein (16). It is entirely feasible to treat even larger molecules within the context of KEM capabilities. Therefore, we performed an ab initio KEM study of the protoribosome and showed that its existence is quite feasible. Using KEM we address the question of whether the basic symmetric structure of the folded dimer pocket that constitutes the protoribosome suggested previously (4) proves to be quantum mechanically stable. If so, the next question to address is: Can it accommodate a pair of amino acids bound to a chain of a few (1–3) nucleotides, representing the tRNA 3′−end, spatially

Significance

The ribosome is essential to life as it functions as "the protein factory" that translates the genetic code into proteins. A universally conserved region around its major active site, where the nascent proteins are being created, was identified in all contemporary ribosomes. Thus, it seems to be a remnant of an entity from the prebiotic RNA world, hence called the "protoribosome." Using quantum mechanics and crystal coordinates of this region, we aimed at answering the question of whether the putative protoribosome has properties essential to function as an evolutionary precursor to the modern ribosome. Our findings show that the necessary conditions that would characterize a practicable protoribosome, namely energetic structural stability and energetically stable attachment to substrates, are well satisfied.

Author contributions: L.M. designed research; L.H. performed research; L.H. and L.M. contributed new reagents/analytic tools; L.H., M.K., A.B., A.Y., and L.M. analyzed data; and A.Y. and L.M. wrote the paper.

The authors declare no conflict of interest.

Freely available online through the PNAS open access option.

[1]To whom correspondence should be addressed. E-mail: ada.yonath@weizmann.ac.il.

This article contains supporting information online at www.pnas.org/lookup/suppl/doi:10.1073/pnas.1314112110/-/DCSupplemental.

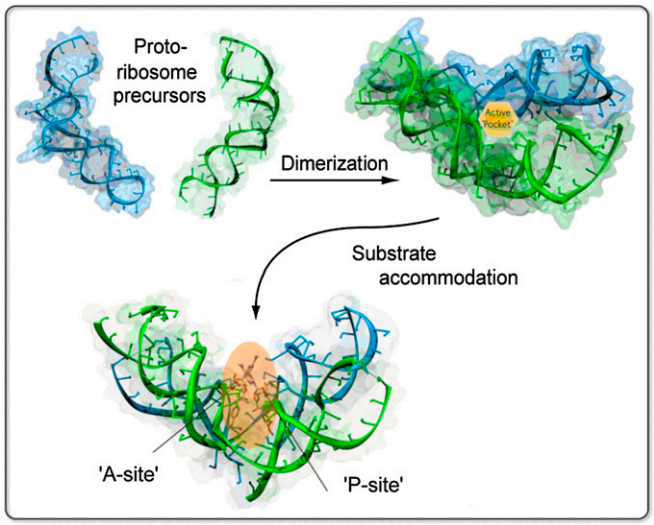

Fig. 1. The scheme by which small, self-folded RNA molecules dimerize to form a symmetrical pocket allowing accommodation of a pair of substrates. The A-site region (Areg) and the P-site region (Preg), respectively, (*Upper Left*) dimerize (*Upper Right*) to allow substrate accommodation. Reproduced by permission from ref. 2 [Davidovich et al. (2009) *Research in Microbiology* 160(7):487–492]. Copyright Elsevier Masson SAS.

and energetically? Furthermore, such calculations should indicate the energetic preferences for the length of the nucleotide chain and its correlation to the protoribome size, ranging between 120 and 180. If both questions would be validated quantum mechanically, that would be highly suggestive of the protoribosome as an actual remnant from the RNA world still functioning in the chemistry of life, in the modern DNA/RNA/protein world.

Results

The quantum calculations discussed here involve 6,019 atoms (including H atoms). We started from the crystallographic atomic coordinates, attached cytosine-cytosine-adenine (CCA)-puromycin molecules to the crystallographic peptidyl-tRNA binding site (P-site) region (Preg) and aminoacyl-tRNA binding site (A-site) region (Areg), after which were appended all of the hydrogen atoms required to satisfy the valences of the various atoms. Our quantum KEM, designed specifically to handle the large number of atoms characteristic of biological structures, was used to do the calculations. The underlying quantum mechanical chemical model used is density functional theory (DFT) with a reasonable basis of atomic orbitals called 3–21*. The results of such a chemical model are reliable as regards energetic trends. To interpret the results, notice that negative interaction energy implies an attractive interaction between components. The results show that the Areg and Preg RNAs have an attractive binding interaction and also both substrates are bound to their RNA sites. The overall conclusion is that the protoribosome structure is energetically stable—that is, the various parts are bound together. In what follows we consider the calculation results for an assumed assembly of the protoribosome in four different cases.

First we consider the RNA object that was mathematically isolated from the heart of the contemporary ribosome, which we call the "180 protoribosome." This includes about 180 nucleotide elements that are conforming to the twofold symmetry in the modern ribosome. The protoribosome with a total of 5,759 atoms consists of an RNA Preg and an RNA Areg, each of which may have substrates attached. In our calculation, the substrates are cytosine-cytosine-puromycins (CCP), each with 260 atoms, one at each Areg and Preg. All of these components are shown in Fig. 2, together with the interaction energies between the various components. The Areg and Preg of the protoribosome are bound to each other with an interaction energy of –1,10.38 kcal/mol. The Areg is bound to its substrate CCPuromycin with an interaction energy of –91.57 kcal/mol. The analogous binding of the Preg to its substrate is –48.06 kcal/mol. Accounting for the "crossing" interactions between the Areg and Preg and the substrates bound to the opposite site, the interactions are smaller at +0.98 kcal/mol and –8.77 kcal/mol, respectively. The interaction between the two bound substrates equals –4.83 kcal/mol. The sum of all interaction energies among all components of the protoribosome with its two substrates attached amounts to –262.63 kcal/mol.

Second we consider how the interactions may change if we reduce the size of the protoribosome and also the size of its substrates. Stripping away 57 of the nucleotides, we term the reduced structure to be a minimal protoribosome of 3,924 atoms called the "120-nucleotide minimal protoribosome," which can, according to our structural analysis, accommodate the last one or two nucleotides at the 3′-end of the aminoacylated tRNA, and the substrates are as before CCP aminoacyl (A) and CCP peptidyl (P), each containing 260 atoms. The minimal protoribosome and its substrates are pictured in Fig. 3, which retains the pattern previously set out in Fig. 2. The analogous interaction energies are as follows. The Areg and Preg of the minimal protoribosome are bound to each other with an interaction energy of –89.65 kcal/mol. The Areg is bound to its substrate CCP with an interaction energy of –37.26 kcal/mol. The analogous binding of the Preg to its substrate is –7.63 kcal/mol. Accounting for the crossing interactions between the Areg and Preg and the substrates bound to the opposite site, the interactions are smaller at +1.42 kcal/mol and –8.89 kcal/mol, respectively. The interaction between the two substrates at the A- and P-sites equals –4.83 kcal/mol. The sum of all interaction energies among all components of the minimal protoribosome with its two substrates attached amounts to –146.84 kcal/mol.

In the third case, we maintain the geometry of the same minimal ribosome as in the second consideration above, but the substrates are reduced to cytosine puromycin (CP) A and CP P, each containing 202 atoms. The minimal protoribosome and its substrates are shown in Fig. 4, which retains the pattern previously set out in Fig. 3. The analogous interaction energies are as follows: The Areg and Preg of the minimal protoribosome are bound to each other with an interaction energy of –89.65 kcal/mol.

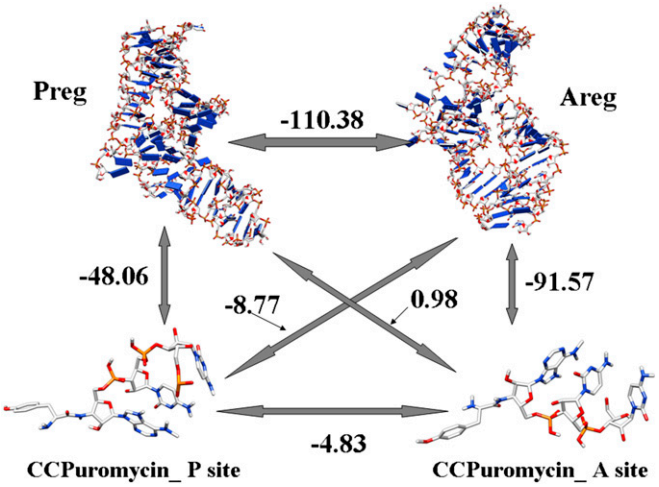

Fig. 2. Interaction energies (Δ), kcal/mol, between pairs of components in the 180-nucleotide protoribosome. The sum of all interaction energies pictured in the figure is equal to –262.63 kcal/mol.

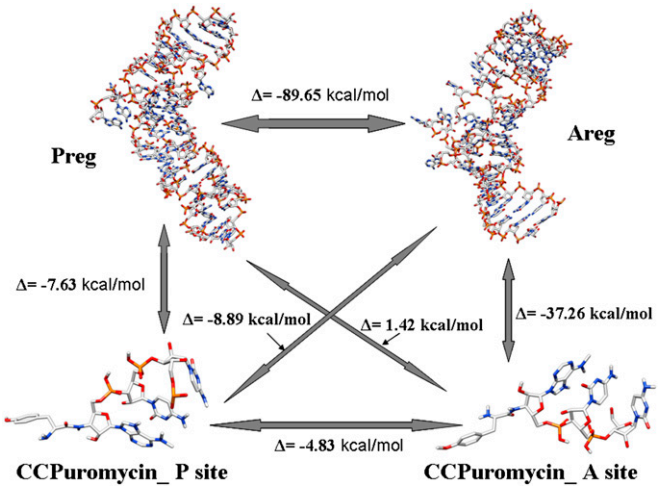

Fig. 3. Interaction energies (Δ), kcal/mol, between pairs of components in the 120-nucleotide minimal protoribosome. The sum of all interaction energies pictured in the figure is equal to –146.84 kcal/mol.

The Areg is bound to its substrate CPuromycin with an interaction energy of –38.48 kcal/mol. The analogous binding of the Preg to its substrate is –9.19 kcal/mol. Accounting for the crossing interactions between the Areg and Preg and the opposite substrates, the interactions are smaller at +2.30 kcal/mol and –9.11 kcal/mol, respectively. The interaction between the two substrates at the A- and P-sites equals –4.20 kcal/mol. The sum of all interaction energies among all components of the minimal protoribosome with its two substrates attached amounts to –148.33 kcal/mol.

Fourth and last, we maintain the geometry of the same minimal 120-nucleotide protoribosome as in the second consideration above, but we reduce the size of the substrates to that of puromycin alone, at both the A- and P-sites, each containing 138 atoms. As before, the minimal protoribosome and its reduced substrates are shown in Fig. 5, which retains the pattern of the previous two figures. The calculated interaction energies are as follows: The Areg and Preg of the minimal protoribosome have the same interaction energy as indicated for them in Fig. 3—that is, –89.65 kcal/mol. The Areg is bound to its substrate Puromycin with an interaction energy of –25.60 kcal/mol. The analogous binding of the Preg to its substrate is –3.72 kcal/mol. The crossing interactions between the Areg and Preg and the opposite substrates are –3.05 kcal/mol and –5.22 kcal/mol, respectively. The interaction between the two substrates at the A- and P-sites equals –4.30 kcal/mol. The sum of all interaction energies among all components of the minimal protoribosome with its two substrates attached amounts to –131.54 kcal/mol.

Table 1 shows all of the numerical values of the interaction energies corresponding to those pictured in Figs. 2–5. The table rows are labeled according to the protoribosome component names, which may be found in Figs. 2–5. The columns are labeled according to the names of the protoribosome and its substrates, whose names also may be found in Figs. 2–5. The seventh row of the table indicates the total interaction energies of the various protoribosomes and substrates attached to them.

Method of Calculations

There are two separate aspects to the calculations we have used. First there is the question of which chemical model we have chosen to use to approximately solve the atomic scale equations of motion—viz., the quantum mechanical Schrodinger equation. A chemical model entails a method of approximation, which in this article is that of DFT (25, 26), and a choice of basis orbitals, in this article 3–21G* (27), which define the Hilbert space for approximation of the molecular orbitals of the molecule studied. The second aspect of the problem is that of the hardware and software used to implement the chemical model that has been chosen. We discuss separately each of these.

The HF approximation (28) is well known and is an often-used ab initio quantum mechanical calculation. It is characterized by use of a single Slater determinant of orbitals, which define a molecular energy minimum within the space of the orbital basis. However, the HF wave function does not include correlation energy, which although small, is sometimes chemically important. Here we use instead DFT, derived from the Hohenberg–Kohn (HK) theorem (25) and its numerical implementation in the Kohn–Sham (KS) equations (26). In common with HF, the DFT/KS wave function is also a single Slater determinant of orbitals. However, KS orbitals deliver the exact electron density, in principle. The KS equations, in form similar to the HF equations, are simpler by way of their potentials, which are of local form. And moreover, the KS potential contains correlation effects, which are absent in the HF approximation. In practice the KS exchange correlation potential is approximated using empirical data and theoretical constraints. DFT KS equations are used in the calculations of this article because of their HF-like simplicity, on the one hand, and their inclusion of correlation, on the other hand.

The calculations referenced above were carried out using Gaussian 09 (29) on the high-performance computer SGI ALTIX, with a parallel computing grid running the UNIX/LINUX operating system. All of the final results of this article have been obtained using the chemical model DFT/B3LYP/3–21G*. Of the many DFT functionals in existence, the DFT/B3LYP approximation is the most widely used. It is a sum of two parts, an empirical Becke 3 parameter exchange contribution (30) and a Lee–Yang–Parr correlation contribution (31) patterned upon the correlations of Colle and Salvetti (32). A reference that shows B3LYP is effective for these systems is that of Lozynski and coauthors (33). The Gaussian basis set 3–21G* (27) combined with B3LYP is expected to be adequate for representations of the protoribosome in this article. As is well known, Pople and his school developed the 3–21G* basis set to reproduce the larger 6–31G* basis set calculated geometries of a test set of molecules.

The DFT chemical model we apply has a computational difficulty that at best rises with the third power of the number of basis functions used. The protoribosome calculations here envision a number of atoms as high as 6,019. Thus, the calculations within the chemical model used would be almost prohibitive, unless a way of simplifying them is used. For this reason the quantum mechanical KEM is used to simplify the computational difficulty, while still retaining the accuracy inherent in the chemical model being used. We give a brief review of KEM.

KEM combines knowledge of atomic coordinates together with the formalism of quantum mechanics. Central to KEM is the kernel concept. Kernels are quantum fragments that summed together constitute a full molecule. Quantum mechanics is applied to only kernels and double kernels, but not a full molecule. Knowledge of the kernels allows reconstruction of all

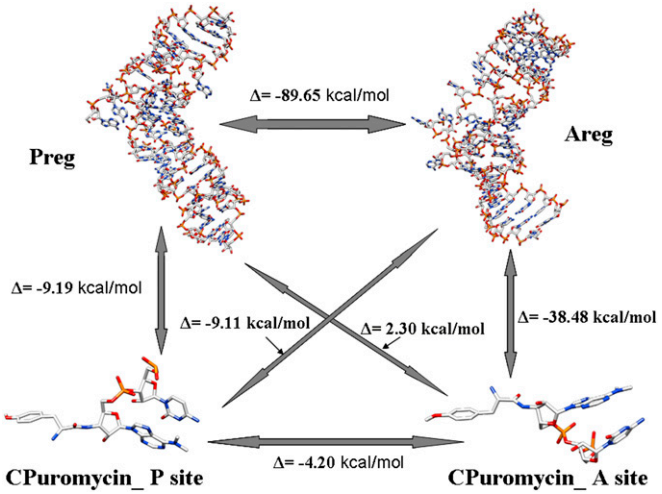

Fig. 4. Interaction energies (Δ), kcal/mol, between pairs of components in the 120-nucleotide minimal protoribosome. The sum of all interaction energies pictured in the figure is equal to –148.33 kcal/mol.

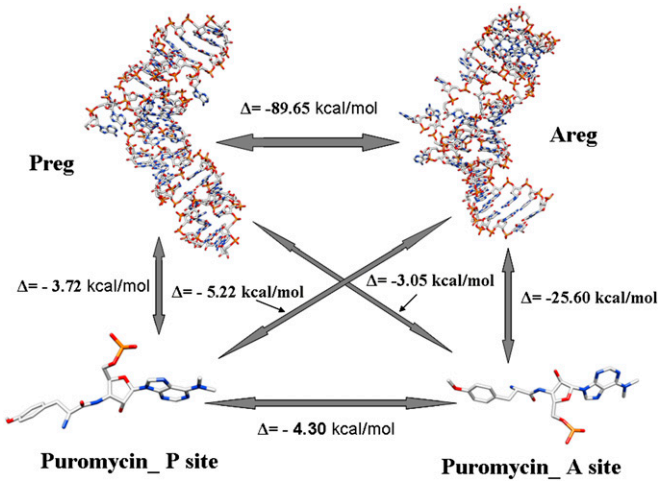

Fig. 5. Interaction energies (Δ), kcal/mol, between pairs of components in the 120-nucleotide minimal protoribosome. The sum of all interaction energies pictured in the figure is equal to –131.54 kcal/mol.

properties of a full molecule. Given a known molecular structure, it is mathematically broken into fragment kernels, whose atomic coordinates are given, such that each and every atom occurs in only one kernel. The total molecular energy is calculated by summation over the energy contributions of the kernels. In KEM, the fragment calculations are carried out on kernels whose ruptured bonds have been capped by the attachment of H atoms to preserve their valence. The contributions of hydrogen caps tend to be negligible, as the caps attached to double and single kernels, respectively, cancel by entering the total energy summation with opposite signs. The total energy is

$$E_n^{total} = \sum_{\substack{i=1 \\ i<j}}^{n-1} E_{ij} - (n-2)\sum_{i=1}^{n} E_i, \qquad [1]$$

where E_{ij} is the energy of a double kernel of name ij and E_i is the energy of a single kernel of name i. The symbols i and j are running indices and n is the number of single kernels. The validity of this has been shown in previous works (8–24). In this article we use the reliable accuracy of KEM to calculate the interaction energies associated with putative protoribosome molecules. The definition of interaction energy between pairs of kernels is:

$$I_{ij} = E_{ij} - E_i - E_j, \qquad [2]$$

where the subscript indices name the pair of kernels in question, I_{ij} is the pair interaction energy, E_{ij} is the energy of a double kernel, and E_i and E_j are each the energies of a single kernel. The sign of the interaction energy, I_{ij}, indicates whether the kernels i and j attract (negative I) or repel (positive I).

The total interaction energy is a sum of the pair of interaction energies of the individual double kernels. The magnitude of a given pair interaction energy I_{ij} determines its relative importance to the total molecular interaction energy. The magnitude of the interaction energies flows naturally from implementation of the KEM, which delivers the ab initio quantum mechanical interaction energy between and among molecular kernels. And this is computationally practical for molecular structures containing thousands or even tens of thousands of atoms.

In using the KEM, we have divided the protoribosome composed of 178 nucleotides and CCPuromycin, in total containing 6,019 atoms, into 60 single kernels. The Preg is made of 29 kernels, and similarly the Areg is made of 29 kernels. The substrates at either the P-site or the A-site, whether CCPuromycin or CPuromycin or Puromycin, are in each case represented as one kernel. The Preg and Areg each consist of several fragments. These are listed in Table S1.

We have calculated the energy of each single kernel and double kernel and subsequently used Eq. **1** to obtain the total energy for RNA and CCPuromycin, and using Eq. **2** we obtained all of the various interaction energies between and among various parts of the putative protoribosomes, as illustrated in Fig. 2. We also have calculated the total interaction energies that stabilize the whole protoribosome system, including substrates.

The minimal protoribosome is suggested to be composed of 120 nucleotides containing 3,924 atoms, which have been divided into 43 kernels. Additionally, CPuromycin at the A- and P-sites together contain 202 atoms and represent an additional two kernels. Puromycin at the A- and P-sites together contain 138 atoms and represent an additional two kernels. The same method as discussed above in relation to Fig. 2 has been used to calculate the total energy and interaction energies illustrated in Figs. 3–5.

Discussion and Conclusions

The primary chemical function of the ribosome is the formation of peptide bonds according to the genetic code. The various complex tasks of the modern ribosome—namely, decoding the genetic code, polymerization of amino acids, protection of the nascent proteins, and responding to cellular signals—dictate its enormous magnitude and complexity and indicate that it must have evolved from simpler molecular precursors. Surely, it is of high scientific interest to reconstruct its possible origin, before describing steps of evolution that may have led to the emergence of the contemporary ribosome. Structural analysis of the 3D structures of ribosomes from the three kingdoms of life has led to a suggestion of what such a precursor might be. We identified a region around the peptide bond formation site that contains a geometrical twofold rotational symmetry. This small universal region (3–4% of the prokaryotic and eukaryotic ribosomes, respectively), in an otherwise gigantic, completely unsymmetrical molecular machine, has been suggested to be a protoribosome precursor (1–3). We assume necessary (although not sufficient) conditions that a true protoribosome must be minimally capable of include (*i*) energetic structural stability and (*ii*) energetic stable attachment to substrates that can ultimately lead to formation of peptide bonds needed for production of proteins. These characteristics of the suggested protoribosome are currently

Table 1. The interaction energies (kcal/mol)

No.	ΔE, kcal/mol	180-nucleotide protoribosome and CCPuromycin (Fig. 2)	120-nucleotide protoribosome and CCPuromycin (Fig. 3)	120-nucleotide protoribosome and CPuromycin (Fig. 4)	120-nucleotide protoribosome and Puromycin (Fig. 5)
1	ΔE_{RNA}(P–A)	−110.38	−89.65	−89.65	−89.65
2	ΔE(Preg–aaP)	−48.06	−7.63	−9.19	−3.72
3	ΔE(Areg–aaP)	−8.77	−8.89	−9.11	−5.22
4	ΔE(Preg–aaA)	0.98	1.42	2.30	−3.05
5	ΔE(Areg–aaA)	−91.57	−37.26	−38.48	−25.60
6	ΔE_{aa}(P–A)	−4.83	−4.83	−4.20	−4.30
7	Total interaction energy	−262.63	−146.84	−148.33	−131.54
8	ΔE(RNA–aaP)	−56.83	−16.52	−18.30	−8.94
9	ΔE(RNA–aaA)	−90.59	−35.84	−36.18	−28.65
10	ΔE(RNA–aa)	−147.42	−52.36	−54.47	−37.58

The seventh row displays the total interaction energies (*SI Appendix*).

being studied experimentally. However, an analogous quantum mechanical study based upon crystallographically determined atomic coordinates, as reported in this article, has not been undertaken in parallel. The two characteristics above are found in this theoretical study to be operative in the putative protoribosome that has been studied.

The dual criteria mentioned above as characteristic of a possible protoribosme have been studied at four levels, which have been demonstrated in Figs. 2–5, and the results have been collected in Table 1. The calculations demonstrated in Fig. 2 indicate that the protoribosome as a whole, on its own, or including its two substrates is an energetically bound molecular system. The same conclusion applies to the minimal ribosome and its three sets of substrates, which are displayed in Figs. 3–5. As indicated in the seventh row of Table 1, the total binding energy of the four cases studied increases with increasing substrate size. This may possibly correlate with the direction of their evolution. However, the main conclusion of this article is that the protoribosome, insofar as it has been studied to this point, may be said to be consistent with the two requirements of energetic stability enumerated.

Inasmuch as one may ask, "How is it that gas phase calculations using crystallographic coordinates can give information on a system in aqueous solution?" we offer in response a *ceteris paribus* argument. Because the dimers and substrates of the calculations are all neutral species, solvent effects should act similarly in the average and so cancel in the energy difference calculations.

Future contributions that can be expected to proceed from quantum calculations would include a search for the transition state (TS) for formation of a peptide bond (34) that would be associated with the protoribosome. There, and as in the calculations of this article, the computational efficiency of KEM will prove to be useful.

Lastly, we mention in passing remarks about the difference between the interaction energy of the aa-mimic at the A-site versus that at the P-site, and in particular what is the significance, if any, of the greater interaction at A- versus that at P-sites. This observation seems to have two aspects, one of which is physical and one of which is biological. Of course, in the end, it is a mandate that both aspects must correspond to what is known experimentally. The physical situation is that the atomic configuration at the P-site differs from that at the A-site. If so, then it is reasonable that the interactions, I, of the aa within the sites would also differ. The fact that I is greater at A than at P is simply a result of the atom configurations adopted and the quantum model used. The results as stated are consistent with the atom positions and the quantum model used. As regards the biology, although it is known that the P-site substrate binds to the contemporary ribosome before the A-site binding, our quantum results obtained thus far do not contradict that. We have calculated the energies of the protoribosome filled with its two substrates. We have also calculated the energies of the protoribosome alone and the free aa's. The difference between these energies is the interaction energies. If one thinks of all this as a chemical reaction with reactants becoming products, we have essentially calculated the energy difference of products and reactants. Such energy differences relate to stability but do not relate to the rates at which the A-site versus P-site would be occupied. Such rates are controlled by the TS of each of the reactions, binding A-site or P-site. The interaction energies of our article are related to the energetic stability of molecules, whereas it would be the activation energy (Ea) of the TS for the chemical reaction leading to chemical products that controls the rate of reaction. The point is that it is entirely possible that the P-site reaction can have a smaller Ea than the A-site reaction, which would correspond to earlier binding to P-site, but simultaneously it can also have a smaller stability than A-site. We do not know if that is the case, because we have not calculated the TS for these reactions. However, the fact that the binding at the P-site is less stable than that at the A-site does not contradict the biology (rates have not been addressed here). Future calculation of the TSs is indicated, along the lines previously published (34). However, it would be a major calculation to undertake, because of the size of the protoribosome, and is not to be included here. The important thing is that our calculated smaller interaction energy at the P-site versus that at the A-site does not contradict rates associated with the P-site versus those of the A-site. There may even be some biological advantage to a relatively smaller interaction energy at the P-site, one may suppose as speculation, because the tRNA has to be pushed out of the P-site into the exit site and it is known that the A-site accommodation of tRNA substrate in the contemporary protein biosynthesis is a rate-limiting step (35).

ACKNOWLEDGMENTS. We thank Paul Whitford for helpful communication. L.H. was funded by the Office of Naval Research through the Naval Research Laboratory's Basic Research Program. L.M. was funded by the US Naval Research Laboratory (Project 47203-00 01) and by a Professional Staff Congress City University of New York Award (Project 63842-00 41). M.K is supported by the Adams Fellowship Program of the Israel Academy of Sciences and Humanities. Funding was received from the European Research Council FP7/2007-2013/ERC Grant 322581. A.Y. holds the Martin and Helen Kimmel Professorial Chair.

1. Agmon I, Bashan A, Zarivach R, Yonath A (2005) Symmetry at the active site of the ribosome: Structural and functional implications. *Biol Chem* 386(9):833–844.
2. Davidovich C, Belousoff M, Bashan A, Yonath A (2009) The evolving ribosome: From non-coded peptide bond formation to sophisticated translation machinery. *Res Microbiol* 160(7):487–492.
3. Krupkin M, et al. (2011) A vestige of a prebiotic bonding machine is functioning within the contemporary ribosome. *Philos Trans R Soc Lond B Biol Sci* 366(1580): 2972–2978.
4. Ben-Shem A, et al. (2011) The structure of the eukaryotic ribosome at 3.0 Å resolution. *Science* 334(6062):1524–1529.
5. Rabl J, Leibundgut M, Ataide S-F, Haag A, Ban N (2011) Crystal structure of the eukaryotic 40S ribosomal subunit in complex with initiation factor 1. *Science* 331(6018):730–736.
6. Bokov K, Steinberg S-V (2009) A hierarchical model for evolution of 23S ribosomal RNA. *Nature* 457(7232):977–980.
7. Line MA (2005) A hypothetical pathway from the RNA to the DNA world. *Orig Life Evol Biosph* 35(4):395–400.
8. Huang L, Massa L (2012) Quantum kernel (KEM) applications in biochemistry, a review paper. *Future Medicinal Chemistry* 4(11):1479–1494.
9. Huang L, Bohorquez H, Matta C-F, Massa L (2011) The kernel energy method: Application to graphene and extended aromatics. *Int J Quantum Chem* 11(15):4150–4157.
10. Huang L, Massa L (2011) Kernel energy method applied to an energetic nitrate ester. *Int J Quantum Chem* 111(10):2180–2186.
11. Huang L, Massa L (2010) The kernel energy method: Construction of 3 & 4 tuple kernels from a list of double kernel interactions. *Theochem* 962(1-3):72–79.
12. Huang L, Massa L (2010) Kernel energy method: Drug-target interaction energies for drug design. *Int J Quantum Chem* 110(15):2886–2893.
13. Weiss S-N, Huang L, Massa L (2010) A generalized higher order kernel energy approximation method. *J Comput Chem* 31(16):2889–2899.
14. Huang L, Massa L, Karle J (2010) *Quantum Biochemistry*, ed Matta CF (Wiley-VCH, Weinheim, Germany), pp 3–60.
15. Huang L, Massa L, Karle I, Karle J (2009) Calculation of strong and weak interactions in TDA1 and RangDP52 by the kernel energy method. *Proc Natl Acad Sci USA* 106(10): 3664–3669.
16. Huang L, Massa L, Karle J (2009) Kernel energy method applied to vesicular stomatitis virus nucleoprotein. *Proc Natl Acad Sci USA* 106(6):1731–1736.
17. Huang L, Massa L, Karle J (2008) The kernel energy method of quantum mechanical approximation carried to fourth-order terms. *Proc Natl Acad Sci USA* 105(6):1849–1854.
18. Huang L, Massa L, Karle J (2007) Kernel energy method: The interaction energy of the collagen triple helix. *J Chem Theory Comput* 3(4):1337–1341.
19. Huang L, Massa L, Karle J (2007) Drug target interaction energies by the kernel energy method in aminoglycoside drugs and ribosomal A site RNA targets. *Proc Natl Acad Sci USA* 104(11):4261–4266.
20. Huang L, Massa L, Karle J (2006) The kernel energy method: Application to a tRNA. *Proc Natl Acad Sci USA* 103(5):1233–1237.
21. Huang L, Massa L, Karle J (2006) The kernel energy method: Basis functions and quantum methods. *Int J Quantum Chem* 106(2):447–457.
22. Huang L, Massa L, Karle J (2005) Kernel energy method: Application to DNA. *Biochemistry* 44(50):16747–16752.

23. Huang L, Massa L, Karle J (2005) Kernel energy method: Application to insulin. *Proc Natl Acad Sci USA* 102(36):12690–12693.
24. Huang L, Massa L, Karle J (2005) Kernel energy method illustrated with peptides. *Int J Quantum Chem* 103(6):808–817.
25. Hohenberg P, Kohn W (1964) Inhomogeneous electron gas. *Phys Rev* 136:B864–B871.
26. Kohn W, Sham L-J (1965) Self-consistent equations including exchange and correlation effects. *Phys Rev* 140:A1133–A1138.
27. Binkley J-S, Pople J-A, Hehre W-J (1980) Self-consistent molecular orbital methods. 21. Small split-valence basis sets for first-row elements. *J Am Chem Soc* 102(3): 939–947.
28. Roothaan CCJ (1951) New developments in molecular orbital theory. *Rev Mod Phys* 23:69–89.
29. Frisch M-J, et al. (2010) *Gaussian 09* (Gaussian Inc, Wallingford, CT).
30. Becke A-D (1993) Density-functional thermochemistry.III. The role of exact exchange. *J Chem Phys* 98:5648–5652.
31. Lee C, Yang W, Parr R-G (1988) Development of the Colle-Salvetti correlation-energy formula into a functional of the electron density. *Phys Rev B* 37:785–789.
32. Colle R, Salvetti O (1975) Approximate calculation of the correlation energy for the closed shells. *Theor Chim Acta* 37:329–334.
33. Lozynski M, Rusinska-Roszak D, Mack H-G (1998) Hydrogen bonding and density functional calculations: The B3LYP approach as the shortest way to MP2 results. *J Phys Chem A* 102(17):2899–2903.
34. Gindulyte A, et al. (2006) The transition state for formation of the peptide bond in the ribosome. *Proc Natl Acad Sci USA* 103(36):13327–13332.
35. Gromadski K-B, Rodnina M-V (2004) Kinetic determinants of high-fidelity tRNA discrimination on the ribosome. *Mol Cell* 13(2):191–200.